Seasonal Variability of Middle Latitude Ozone in the Lowermost Stratosphere Derived from Probability Distribution Functions

Richard B. Rood
Data Assimilation Office, Code 910.3
NASA Goddard Space Flight Center
Greenbelt, MD 20771
rrood@dao.gsfc.nasa.gov
301-614-6155

Anne R. Douglass
Atmospheric Chemistry and Dynamics Branch, Code 916
NASA Goddard Space Flight Center
Greenbelt, MD 20771

Mark C. Cerniglia
Atmospheric and Environmental Research, Inc.
840 Memorial Drive
Cambridge, MA 02139-3794

Lynn C. Sparling
University of Maryland, Baltimore County
@ Atmospheric Chemistry and Dynamics Branch, Code 916
NASA Goddard Space Flight Center
Greenbelt, MD 20771

J. Eric Nielsen
SM&A Corporation
@ Atmospheric Chemistry and Dynamics Branch, Code 916
NASA Goddard Space Flight Center
Greenbelt, MD 20771

Seasonal Variability of Middle Latitude Ozone in the Lowermost Stratosphere Derived from Probability Distribution Functions

R. B. Rood, A. R. Douglass, M. C. Cerniglia, L. C. Sparling, and J. E. Nielsen

Abstract. We present a study of the distribution of ozone in the lowermost stratosphere with the goal of characterizing the observed variability. The air in the lowermost stratosphere is divided into two population groups based on Ertel's potential vorticity at 300 hPa. High (low) potential vorticity at 300 hPa indicates that the tropopause is low (high), and the identification of these two groups is made to account for the dynamic variability. Conditional probability distribution functions are used to define the statistics of the ozone distribution from both observations and a three-dimensional model simulation using winds from the Goddard Earth Observing System Data Assimilation System for transport. Ozone data sets include ozonesonde observations from northern midlatitude stations (1991-96) and midlatitude observations made by the Halogen Occultation Experiment (HALOE) on the Upper Atmosphere Research Satellite (UARS) (1994-1998). The conditional probability distribution functions are calculated at a series of potential temperature surfaces spanning the domain from the midlatitude tropopause to surfaces higher than the mean tropical tropopause (~380K). The probability distribution functions are similar for the two data sources, despite differences in horizontal and vertical resolution and spatial and temporal sampling. Comparisons with the model demonstrate that the model maintains a mix of air in the lowermost stratosphere similar to the observations. The model also simulates a realistic annual cycle. Results show that during summer, much of the observed variability is explained by the height of the tropopause. During the winter and spring, when the tropopause fluctuations are larger, less of the variability is explained by tropopause height. This suggests that more mixing occurs during these seasons. During all seasons, there is a transition zone near the tropopause that contains air characteristic of both the troposphere and the stratosphere. The relevance of the results to the assessment of the environmental impact of aircraft effluence is also discussed.

1. Introduction

The focus of this study is to better characterize the distribution of ozone in the lowermost stratosphere of northern middle latitudes. This layer is the transition region between the stratosphere and troposphere, and conceptual models of transport in either regime break down. The motivation to better understand tracer distributions in the neighborhood of the tropopause is provided by the potential importance of changes in trace composition to issues of both atmospheric chemistry and climate. In particular, since airplanes emit their effluents in the upper troposphere and the lowermost stratosphere, confidence in our ability to assess current or future impact of air traffic on the environment depends on how well we can characterize this region.

Much of our present understanding of constituent distributions in the upper troposphere and lower stratosphere comes from the study of stratosphere-troposphere exchange. Some previous studies have focused on the role of synoptic and sub-synoptic scales that directly perturb the tropopause. Attention has been placed on the dynamics in the vicinity of tropopause folds [*Danielsen,* 1968; *Danielsen et al.*, 1970; *Shapiro,* 1980; *Lamarque and Hess*, 1994; *Langford et al.*, 1996; *Beekmann et al.*, 1997] or associated with cutoff lows [*Bamber et al.*, 1984; *Vaughan and Price,* 1989; *Price,* 1990; *Price and Vaughan,* 1993; *Ancellet et al.*, 1994]. *Zahn et al.* [1999] point out the enormous complexity of trying to understand stratosphere-troposphere exchange from the study of detailed processes near the tropopause, as well as provide an excellent bibliography of recent work in the field.

An alternative global-scale dynamical approach to stratosphere-troposphere exchange was reviewed by *Holton et al.* [1995]. From this perspective Rossby waves and gravity waves generated in the troposphere propagate and dissipate at higher altitudes causing a wave-induced westward zonal force. This force causes a mean meridional mass circulation with upward transport in the tropics and downward transport at high latitudes, especially during winter and spring. Evaluating stratosphere-troposphere exchange by exploiting this principle of "downward-sideways control" does not require specific attention to synoptic-scale disturbances and has often

proven more effective than trying to integrate the net effect of insufficiently characterized individual events. However, *Holton et al.* [1995] point out that transport issues in the lowermost stratosphere, below the 380 K surface, start to violate the assumptions used to develop the downward-sideways control theory, and especially in the case of the impact of aircraft emissions the role of local processes must be evaluated.

Recent three-dimensional investigations of stratosphere-troposphere exchange involve the use of meteorological fields from general circulation models and data assimilation systems. These include: the diagnostic investigation of meteorological analyses [e.g. *Dunkerton*, 1995; *Appenzeller et al.*, 1996b; *Gettelman and Sobel,* 1999]; the use of meteorological analyses in contour advection and trajectory calculations [*Ancellet et al.*, 1994; *Newman and Schoeberl*, 1994; *Appenzeller et al.*, 1996a, *Schoeberl et al.*, 1998]; and the use of mesoscale [*Lamarque and Hess*, 1994; *Ebel et al.*, 1996] and global models [*Mote et al.*, 1994; *Chen,* 1995; *Cox et al.*, 1995; *Rood et al.*, 1997; *Gettelman*, 1998]. These investigations usually focus on specific case studies or seasonal transport simulations, and show that the meteorological analyses and model fields are of sufficient quality to model much of the variability of specific events. However, the extraction of the net transport from the often reversible undulations caused by these individual events remains uncertain.

This study builds on the success of our earlier studies to model tracer variability under the presumption that the mean state is indicative of the net effect of the individual events. We will, therefore, apply statistical methods to link local variability on time scales of days to the global mean state. Conditional probability distribution functions (PDFs) are used to describe the mean state of the constituent distribution. *Sparling* [1999] investigates a variety of stratospheric transport and mixing processes using PDFs and argues that the PDFs provide an important test of model performance. Even though the PDFs calculated from observations do not themselves reveal specific transport mechanisms, if the PDFs from the model fields show realistic small-scale variability we have increased confidence in model performance. Such realism is a prerequisite for the integrated effect of the transport mechanisms to be well represented. We

will investigate the ability of the PDFs to identify information in the observations, and whether or not the model can simulate similar signals.

We focus on ozone to describe the mix of air in the lowermost stratosphere. Ozone serves as a useful tracer because of its long lifetime and the availability of observations (ozonesondes and satellite). While in the mean there is a large increase of ozone from the troposphere to the stratosphere, the ozonesondes show that from day to day, the vertical gradient is not monotonic. We attempt to exploit the information in this structure. The ozonesondes are limited in spatial and temporal coverage; therefore, we also utilize Halogen Occultation Experiment (HALOE) observations from the Upper Atmosphere Research Satellite (UARS). HALOE regularly retrieves ozone profiles down to the tropopause [*Bhatt et al.*, 1999]. Like ozonesonde profiles, HALOE profiles show a high degree of variability in the lowermost stratosphere. We use the PDFs to establish consistency between the two observation types, and then apply the same sampling and statistical methods to the model to evaluate the model performance. Section 2 describes the ozone data sets. The model and experimental set up are described in Section 3. The analysis method and its application to both the observations and the simulations are given in Section 4. Section 5 discusses the results, and the final section is a summary.

2. Ozone Datasets

2a. Ozonesondes

Profile data from fifteen ozonesonde stations located between 42 N and 60 N for the years 1991 through 1996 are used to establish averaged statistics. The vertical resolutions of the sonde profiles are on the order of a few hundred meters in the lower stratosphere. The accuracy of the observations is ~5% in the lower stratosphere and ~10% in the troposphere [see *Bruhl et al.*, 1996, and references therein]. The balloon launch frequency of the European stations is much greater than at stations in Asia or North America, and the stations are not uniformly distributed.

Due to possible preferential locations of dynamical features that cause ozone variability, biases in the observations due to spatial sampling are potentially important. For instance, *Beekmann et al.* [1997] investigated tropopause-folding activity using 10 years of the European Center for Medium-range Weather Forecasting (ECMWF) analysis and determined that regions in Europe and east of North America and Asia were areas of maximum folding activity. *Ebel et al.* (1996) performed a similar analysis and extended it to include global cutoff low activity. They showed a geographical preference for cutoff low formation similar to that for folds with higher frequencies over landmasses [see also, *Price and Vaughan*, 1993; *van Haver et al.*, 1996]. The ozonesonde network, therefore, samples the regions of maximum tropopause fold and cutoff low activity. We evaluated any bias this sampling preference might have on this study and conclude that the results are not corrupted by the geographical proximity of sonde launches to persistent weather patterns.

2b. Halogen Occultation Experiment (HALOE)

Level 2 HALOE ozone profile data from 1994 through August 1998 are used to construct a second set of averaged statistics. HALOE makes a total of approximately 30 sunrise and sunset occultation measurements at two latitudes per day. We select the HALOE data from the same 42 N to 60 N latitude bands of the ozonesonde data. Since HALOE observations are equally spread in longitude, they allow us to investigate any impact the fixed longitudinal distribution of the ozonesonde stations might have. HALOE observations prior to 1994 are omitted from this study because Pinatubo aerosols prevented accurate observation of constituents in the lower stratosphere. The vertical resolution of HALOE is approximately 2 kilometers and the horizontal footprint is approximately 120 kilometers. HALOE ozone channel mixing ratio error estimates are ~10% in the mid-stratosphere and ~30% near 100 hPa [*Russell* et al., 1993; *Bruhl et al.*, 1996]. A quality control procedure, based on the standard deviation of the data, is implemented in our analysis to determine the lowest reliable height of each sampled profile. This procedure indicates that the lower observation limit of HALOE is approximately the height of the

tropopause. Because convective clouds patterns might have different characteristics over land than ocean, we have attempted to discern any land-sea bias in whether or not the profiles reach the tropopause. We did not find any signal.

As part of the UARS ozone validation, *Bruhl et al.* [1996] made comparisons of 100 HALOE and ozonesonde profiles and reported that there was agreement in most cases. Root-mean-square differences appeared largest in winter and spring due to increased atmospheric variability. In a direct comparison of 30 summer and winter sonde profiles from Hohenpeissenberg (47.8N, 10E) and HALOE (mean latitude of 47.7N), *Bruhl et al.* [1996] showed that agreement was fair in the lower stratosphere though percent differences increased quickly below 100 hPa. Temporal and spatial variability and Pinatubo aerosol contamination represented a large fraction of the error estimate between HALOE profiles and midlatitude correlative measurements. *Bhatt et al.* [1999] performed an extensive evaluation of HALOE and the sonde data and showed that if the HALOE data were properly screened for aerosol effects, that HALOE agreed, on average, within 10% of the sondes. This level of agreement was found down to 200 hPa at middle latitudes. We will show in section 4 that the statistics of the sonde and HALOE data sets are consistent. This is important because of the significant differences in the spatial and temporal sampling of the data sets. Because the statistics of the data sets are consistent, we infer that the variability of each data set is representative of the actual variability in the lowermost stratosphere.

3. Chemistry and Transport Model

The Goddard chemistry and transport model (CTM) uses winds from the Goddard Earth Observing System Data Assimilation System (GEOS DAS) [*Schubert et al.*, 1993] for transport. The model uses a 2.5 longitude by 2 latitude horizontal grid. The vertical domain includes 11 terrain following sigma levels from the surface to 130 hPa and 17 isobaric levels to 0.1 hPa. The vertical resolution in the lower stratosphere is approximately 1 kilometer. Advection is accomplished using the flux-form semi-Lagrangian algorithm of *Lin and Rood* [1996]. The one

year parameterized ozone simulation follows the method described by *Douglass et al.* [1996], using production and loss coefficients taken from the Goddard 2D model [*Jackman et al.*, 1996]; these coefficients are updated every 15 days. An additional global tropospheric loss with an e-folding time of seven days is applied to sigma levels below seven kilometers The time step is 900 seconds. The simulation runs from December 26, 1996 through the end of 1997. The ozone initialization is based on data from the Microwave Limb Sounder on UARS [*Froidevaux et al.*, 1996], as discussed by *Douglass et al.* [1997].

The CTM has been used successfully in a number of studies, which emphasize direct comparison of model fields with observations from sonde, aircraft, and satellite, relying on the information in the assimilation winds to reproduce the planetary and synoptic variability [e.g., *Douglass et al.*, 1996; *Douglass et al.*, 1997 and references therein]. In particular the model has been shown to simulate the variability in constituent distributions caused by dynamical processes near the tropopause [esp. *Cerniglia et al., 1995; Rood et al. 1997*]. The simulations are of sufficient quality that after several months of integration one-to-one correspondence can often be found between modeled and satellite observed synoptic scale variations. However, after several months of integration, biases, which build up in the mean fields, degrade the quantitative utility of the model.

Previous work also provides evidence that the overall transport in the lowermost stratosphere is consistent with CO_2 observations. An analysis of aircraft observations of CO_2 by *Strahan et al.* [1998] shows a change in the phase of the CO_2 annual cycle at the midlatitude tropopause. This change in phase shows that primary path between the troposphere and stratosphere is unlikely to be at middle latitudes. Furthermore, the phase of the annual cycle in CO_2 seen in the lowermost stratosphere at middle latitudes is consistent with horizontal transport of CO_2 from the upper tropical troposphere, thus suggesting the importance of horizontal transport to the composition of the lowermost stratosphere.

A bias that builds up after several months of integration was noted above. The model generally produces high ozone relative to observations in the middle to high latitude lower

stratosphere, particularly during the summer. This discrepancy is not unique to the GSFC CTM [*Park et al.*, 1999], and there is evidence that systematic problems in the mean transport characteristics play a large role in the deficiency of the ozone simulation.. *Hall et al.* [1999] in a general evaluation of models conclude both that the upward transport in the tropics is too rapid and that the mixing between the tropics and the middle latitudes is too strong. Further, numerous authors [e.g. *Waugh,* 1996; *Kindler et al.* 1998; *Weaver et al.*,1999] have shown that the current generation of meteorological analyses overestimate transport out of the subtropics into middle latitudes. Although the comparisons shown here reveal the existence of this high bias, the mix between the tropospheric and stratospheric air in the lowermost stratosphere is not strongly affected by these deficiencies in the stratospheric circulation through the first few months of the integration.

4. Analysis of Observations and Model Output

4a. Definition of Tropopause

The tropopause will be defined by the 2.0 Ertel's potential vorticity (PV) unit (pvu = 10^{-6} m^2 s^{-1} K kg^{-1}) level, which is an accepted dynamical definition of the midlatitude tropopause. There are other definitions of the tropopause based on temperature or ozone. These are necessary in the tropics where the PV definition breaks down. Because this study is limited to middle latitudes, the PV definition is adequate. *Bethan et al.* [1996] studied the sensitivity of the determination of tropospheric ozone to the definition of the tropopause. For quantitative purposes, they found that the difference between using the thermal tropopause and ozonopause was quite large. *Gettelman* [1998] studies the sensitivity of aircraft effluent transport to the choice of PV surface used to define the tropopause and found that the stratospheric burden of aircraft pollutant was relatively insensitive to choice of the tropopause definition. Since the focus of this paper is to identify whether the air is of tropospheric or stratospheric character, the results are relatively insensitive to the chosen definition of the tropopause.

4b. Overview of Observed and Modeled Ozone Variability

A year-long record of ozonesonde observations at the Hohenpeissenberg station (47.8 N, 11 E) is shown in Figure 1 along with a similar record taken from the CTM. The sonde observations are interpolated to constant potential temperature surfaces, using *in situ* potential temperature profiles from the sondes. The annual mean is subtracted from the record in order to emphasize the variability and facilitate comparison between the simulation and the observations. The balloon launch dates are marked with a "+" below the x-axis. The tick marks indicate the 1st and 15th of each month; the tick marks indicating the 15th are annotated. The top of the lowermost stratosphere is defined by the 380K potential temperature isentrope and the bottom is defined by the 2-pvu tropopause. Both are marked in white. The standing mix of many local ozone maxima and minima is evident. This variability is typical of northern midlatitude stations.

The information from the simulation is plotted by taking profiles from the same location as the Hohenpeissenberg station and interpolating them to constant potential temperature surfaces. For this case, potential temperature from the GEOS DAS analysis is used. By plotting the anomaly from the annual mean, the bias between the model and the observations is obscured, and the variability is more easily compared.

The impression from this comparison is that the model is faithful to the observations in its depiction of the lower stratospheric ozone variability. There are generally positive anomalies from February through June and negative anomalies from July through January. The quality of the model integration starts to suffer by November, when the simulation shows the return of positive anomalies. The exact source of this discrepancy is not yet understood; though, it is probably related to the biases in the mean ozone gradient that develop in the integration. During the winter and spring the magnitude of the episodic variability is well simulated, as well as seasonal transition from June to July. The simulation represents the frequency of the variability in summer; however, the modeled magnitude of the anomalies in the summer and fall is larger than observed. In both model and observations, there is evidence of variability up to 500K, the highest level shown.

4c. Representativeness of Data Sources

Probability density functions (PDFs) will be used to quantify the variability in observed and modeled O_3 [*Sparling,* 1999]. A PDF is defined for a 10 nbar ozone partial pressure bin size. For a distribution with N total observations, the value of the PDF for a given ozone range is the number of occurrences within that range divided by N and expressed as a percent. The model fields are available every six hours at regular intervals of latitude and longitude. Sonde profiles are available at fixed locations at 3-5 day intervals. HALOE provides about 15 profiles equally spaced in longitude at two latitudes each day. In the latitude range used in this study (42-60 N) there are usually 10 or more successive days of observations each month. There are similar length periods with no observations.

There are several aspects of spatial and temporal sampling that must be addressed. First, it is important to determine how many samples are required to assure stable statistics. In Figure 2 we compare PDFs for model ozone at 350K at the location of the Hohenpeissenberg station. The crosshatched area shows the PDF for daily sampling; the bold solid line is the PDF for sampling every 5^{th} day. There are clear differences between the two distributions in Figure 2. As the sampling frequency is increased for 1 per 5 days to 1 per 4 days (etc.) the distributions become more similar. The PDF for the model field sampled every second day is nearly identical to the PDF for daily sampling.

Because the sonde observations are provided at most every 3 to 5 days, the model results suggest that over the course of one year the ozonesondes may not adequately define the statistics of the ozone variability. Therefore, all six years (1991-1996) of ozonesonde observations will be used to describe the ozone variability in the lowermost stratosphere. This presumes that the basics of the seasonal behavior exist each year. We test this assumption by comparing distributions made using different combinations of 5 years of sonde observations. The distribution using all six years of observations is nearly identical to the distributions obtained using any set of five years of observations.

We test the dependence of the statistical distribution on spatial sampling by comparing PDFs derived from the sondes with PDFs derived from HALOE. A further test is made by comparing the distribution for the subset of HALOE profiles over the oceans to the subset of HALOE profiles over land. All of these distributions are similar, suggesting that the data sets are representative of the middle latitude lower stratospheric variability.

Finally, the HALOE data set has fewer profiles than the sonde data set. The number of profiles available from the model is much larger than either of the observational datasets. To account for this disparity, we randomly select from the model and ozonesonde data set the same number of profiles available from HALOE. As above, the distribution using all six years of ozone sonde observations is nearly identical to distributions using these random subsets of ozonesonde profiles.

4d. Conditional Probability Distribution Functions (PDFs)

Previous model experiments reveal that much of the episodic variability in both the model and the observations is linked to the dynamical variability associated with Rossby waves of both planetary and synoptic scale. Much of the transport associated with these waves is reversible, and specifically linked to the rise and fall of the tropopause. In order to account for variability caused by these large undulations, the analysis technique used here partitions the ozone based on the distribution of potential vorticity and, *de facto*, tropopause height. This also means that the ozone observations from similar synoptic situations are being grouped together. Therefore, even though coincident space and time comparisons are not possible across the multi-year data sets, we are comparing observations that should be similarly effected by dynamical processes.

At any given time the potential vorticity is a complex function of latitude and longitude, which is illustrated in Figure 3, which shows contour maps of isobaric PV at 300 hPa for days representative of MAM (April 1, 1997) and JJA (July 12, 1997). The 2-pvu contour (bold) marks the intersection with the tropopause. The PV distributions for DJF and SON are similar to MAM

and are not shown. The 300 hPa surface is chosen because it approximates the height of the annual midlatitude tropopause [*Morgan and Nielsen-Gammon*, 1998]. Broadly, during MAM (Figure 2a) there is high PV at high latitudes and low PV at low latitudes. Since PV increases rapidly with altitude above the tropopause, high PV is correlated with a low tropopause and *vice versa*. The high latitude PV represents the cyclonic vortex over the pole, which is stronger in the winter and weaker in the summer. There are a number of high PV events, many traversing the middle latitudes that coincide with spatial scales of hundreds to 2000 km. These cyclonic scales, which include folds and cutoff lows, constantly distort and displace the local tropopause and perturb the lower stratosphere and the upper troposphere [see, *Appenzeller*, 1996a]

Figure 3b shows the PV on July 12 and is representative of summertime conditions. In general the tropopause is higher in the summer, consistent with the broadly lower values of PV. In fact, through much of the middle latitudes there is little contrast with the subtropics. Both planetary wave and synoptic wave activity decrease in the summer. The cyclonic systems that are present tend to be isolated from any high latitude PV source. The seasonal transition evident from comparing Figures 3a and 3b is reflected in the ozone data in Figure 1, where, during summer, the tropopause height is observed to increase and there is a substantial reduction of the ozone. Figure 1 also shows that during this summer regime, there does continue to be variability linked to the traveling waves typified in Figure 3b.

In all seasons the distortion associated with different dynamical events juxtaposes air with different tropopause heights. For instance, during MAM (Figure 3a) between - 60 and -120 longitude there is a protrusion of air with low PV, hence high tropopause (marked "H"), to higher than 65 N latitude. Since ozone is much lower in the troposphere than in the stratosphere, traversing this protrusion would show low ozone compared to the two regions of high PV, low tropopause (marked "L"), high ozone on either side. Taking a transect at 48 N, the latitude of Hohenpeissenberg, there would be numerous highs and lows of ozone correlated with the highs and lows in PV. Since these cyclonic scales travel in time, sitting at a single location (*e.g.*,

Hohenpeissenberg), there would be a series of high and lows in the ozone data as the different disturbances passed (see Figure 1).

Figure 3a shows that many of midlatitude high PV systems are attached to high-latitude reservoir. If they detach, animations show that the high PV blobs often rejoin their PV source region at a later time. Assuming that the time scales of tracer sources and sinks are not short compared with PV time scales, this suggests that much of the transport associated with these events is reversible. That is, at a point in middle latitudes, high ozone values are often simply associated with distortions of the polar vortex and the tropopause and represent a transient effect. A similar phenomenon occurs with low PV air masses that can be linked to a tropical and subtropical reservoir. Some features are simply distortions along the subtropical jet stream, some features break free and return, and some features break free and dissipate at latitudes away from their source region. The features that dissipate away from their source regions are most obviously irreversible.

The PV distributions can be compared more quantitatively by calculating PDFs. Here the bin size is 0.5 pvu. The PDF for April 1, 1997 (Figure 4a) shows a broad range of PV values with a relatively large variance that is representative of MAM. The low end of the PV distribution (PV values < 1 pvu) correspond to a low PV background associated with fair weather and subtropical air that is advected to midlatitudes during wave events. At the other end of the distribution, with less probability of occurrence, are PV values in excess of 3 pvu. These high PV values represent strong cyclonic events that are related to the high latitude and stratospheric PV reservoir. The PDF for July 12, 1997 (Figure 4b) shows, as in spring and winter, mostly PV values < 1 pvu. Compared with the April 1 distribution, the July 12 distribution shows more frequent occurrence of PV values in the range 1.5 to 2.5 pvu and no instances of PV greater than 3.5 pvu. The PDFs of potential vorticity show the difference in synoptic activity between summer and the other seasons. The summer is characterized by weaker synoptic-scale storms, and hence, the very high values of PV are not observed.

Ozone from both observations and the model simulation will be divided into two families based on the height of the tropopause as defined by the intersection of the 2-pvu surface with the 300 hPa surface (i.e. Figure 3). In particular, the criterion for a high tropopause air mass is a PV value at 300 hPa of less than 2 pvu at 300 hPa, and the criterion for a low tropopause air mass is a PV value greater than or equal to 2 pvu. Ozone profiles sampled from a high tropopause air mass exhibit a subtropical character. Those from a low tropopause air mass exhibit a more polar character. The extent to which a synoptic event penetrates into the stratosphere has a direct impact on the profile shape at higher altitudes. The PDFs will be calculated for each of these categories. These conditional PDFs should account for dynamical variability present in instantaneous ozone observations. In as much as the statistical distribution represents the mean state, comparison of model with observations provides a test of the ability of a global model to simulate the observed ozone behavior. It also allows for a direct comparison between different ozone observation platforms, namely the ozonesondes and HALOE.

4e. Application to Ozone

Ozone variability is studied by calculating conditional probability functions (PDFs) based on the partitioning defined in the previous section. The PDFs are calculated for the ozonesonde observations, the HALOE observations and the simulation. In much of the lowermost stratosphere, the partitioning based on the PV at 300 hPa divides the observations into nearly equal-size groups for all seasons. Conditional PDFs are presented in Figure 5 for the 350 K isentropic level. This surface is a representative level to examine the seasonal behavior of the ozone variability that exists in the midlatitude lowermost stratosphere (refer to Figure 1a). To facilitate comparison with the model, sonde and HALOE data are interpolated to model pressures. Corresponding potential temperature profiles are calculated using *in situ* profiles in the case of ozonesondes, temperatures from the National Center for Environment Prediction (NCEP) analysis which are coincident with observed ozone profiles in the case of HALOE, and temperatures from the GEOS DAS analysis for the gridded CTM output. The vertical binning

uses 10 K intervals. As discussed in Section 4c, sonde and model profiles are randomly rejected to concur with the number of observations available from HALOE.

Figure 5 shows good agreement between the sonde and HALOE PDFs during all seasons. A broken line represents the observations from the low tropopause group and has generally higher ozone values than the high tropopause group represented by the solid line. In DJF, the most probable ozone partial pressures are nearly equal in the two groups, but the shapes of the distributions differ. The high tropopause group bulges towards low ozone values, and the low tropopause group has more ozone observations with the highest ozone values. In MAM, the peaks of the two groups are more separated, which indicates that during spring that the tropopause partitioning is a more definitive indicator of ozone amount than in the winter. In JJA, the two PDFs are most sharply peaked and distinct from one another, and tropopause height is strongly correlated with ozone amount. In SON, the separation of the two peaks is less distinct, more like the springtime.

There are a number of other notable characteristics of the PDFs from the observations. The seasonal cycle visible in Figure 1 is represented in the PDFs. Consistent with the rise in the height of the tropopause during summer, the most probable value of ozone becomes smaller in both the high tropopause and low tropopause groups. The minimum ozone in each of the populations is during SON. However, the seasonal progression of the two groups differ. For the high tropopause (solid line) case DJF and MAM are quite similar. There is a distinct change from MAM to JJA with a steepening of the PDF and the most probable value decreasing to less than 50 nbar. In both the sonde and HALOE observations the peak becomes even more distinct in SON, with the tail towards high values of ozone lessening.

For the low tropopause case (broken line) there is more significant seasonal change from JJA to SON. As in the high tropopause case, the winter and spring PDFs are similar and there is change going into the summer. The summer change is characterized by the most probable value remaining close to that seen in MAM, but with significant reduction of the number of low values. Then going into SON, the spread of the ozone values decreases and the most probable value

decreases from more than 100 nbar to about 50 nbar. This suggests profiles for the low tropopause group having ozone values more characteristic of tropospheric ozone to higher altitudes in SON. This is consistent with the analysis of Lightweight Airborne Chromatograph Experiment (LACE) data presented by *Ray et al.* [1998], which shows that the vertical profiles of long lived gases such as CFC-11 have a much more tropospheric character in September than in May.

The model behavior (bottom of Figure 5) captures some of the features of the observations. The model peaks show the least separation in DJF and the most separation in JJA. From December through August the most probable value in the simulation is close to that which is observed. The separation of the summertime peak in the model is not as clear as in the observations. Nevertheless, the model is consistent with the observations in that tropopause height explains more of the variability in the summer than in the spring and winter. In SON the model compares less favorably with the observations. Most notably, the low-tropopause/high-ozone group does not show the significant reduction in the most probable ozone value. This is consistent with the return to positive anomalies that was noted in Figure 1, and might be related to the bias that develops in lower stratospheric ozone, especially in the summer.

To illustrate the vertical structure of the ozone variability in the lowermost stratosphere, the seasonal PDFs are shown for JJA at 10 K intervals from 320 K to 430 K are shown in Figure 6. At the lowest level, 320 K, the PDFs of both the high and low tropopause partitions lie on top of each other with ozone values typical of the troposphere. It is safe to say that during summer the air at 320 K is predominately tropospheric, with only a few high values of ozone contributed by the low tropopause group. From 330 K to 380 K the high and low tropopause populations separate into two groups. The maximum peak separation is at 350 K. Air of both stratospheric and tropospheric character resides throughout this altitude range, and, to greater or lesser extents, the tropopause height correlates with the ozone values. Above 380 K the two groups start to overlap more, and by 410 K the PDFs are no longer discriminated by the height of the tropopause. The air above 410 K is stratospheric.

Other seasons (not shown) do not show as clear a separation of the ozone values based on tropopause height as seen during summer. During winter there is significant overlap of the high and low tropopause values at all altitudes. Plus, during winter both of the conditional PDFs show a wide range of ozone values as seen at 350 K in Figure 5. In the springtime, there is a separation of the two families at altitudes below 350 K. In the fall, SON, there is weak separation of the two groups maximizing at 340 K. Since synoptic activity is stronger in winter and spring than in summer (e.g. Figures 3 and 4), the tropopause variability is expected to be stronger and more intense in winter and spring. However, the tropopause is a less certain predictor of lowermost stratospheric ozone in winter and spring, suggesting that air is more thoroughly mixed in winter and spring than in summer.

The behavior of the ozone in the lowermost stratosphere is summarized graphically in Figure 7, where the most probable value of ozone is plotted as a function of potential temperature altitude and time. In this case monthly PDFs were used instead of the seasonal, conditional PDFs presented in Figures 5 and 6. For both the sonde and HALOE observations the seasonal cycle is a discernable function of height. At 440 K the peak ozone occurs around March and the low occurs in August, consistent with the well known stratospheric seasonal behavior. At 340 K the peak occurs in April and the minimum is in September. The amplitude is larger at lower altitudes. Especially in the sonde data there is an abrupt transition in the seasonal pattern near 400 K.

The model, bottom left part of Figure 7, captures some of the observed features. Note that the maximum values of the z-axes differ for the two data sets and the model, as the model values are biased high relative to the observations. Notably, the simulated seasonal cycles at 340 K and 440 K are quite consistent with the observations in both phase and magnitude. The transition around 400 K is not distinct in the model.

5. Discussion

The diagnostics presented in the previous section show that in the transition region between the stratosphere and the troposphere ozone behaves differently than it does at either higher or lower altitudes. Observations have only been studied in northern hemisphere middle latitudes. Notably the seasonal cycle above, approximately, 400 K is smoother than it is right above the tropopause, for instance 350 K. Further, the phase is different in the two regimes, with the maximum occurring about one month later in the lower regime. In the lower regime the transition from spring to summer is much sharper. In the ozonesonde observations, the 400 K transition between the two regimes is definitive. The transition is less clear in the HALOE data, probably related to the lower vertical resolution of the HALOE observations. The model represents the difference between the seasonal cycle observed at the top and bottom of the lowermost stratosphere; however, the model does not represent the transition clearly.

Pan et al. [1997] describe the behavior of both water vapor and ozone in the lowermost stratosphere using satellite observations from the Stratospheric Gas and Aerosol Experiment II (SAGE II). *Pan et al.* [1997] show (their Figure 6) similar behavior to that reported here in the seasonal cycle of ozone, with the peak approximately one month later at 320 K than at 420 K. Also, the summer minimum is more distinct and stretches into autumn at the lower altitude. As the data are presented in *Pan et al.* [1997], it is not possible to discern whether there is a transition altitude as distinct as the one reported here. The water vapor observations also show a change in the characteristic of the seasonal cycle, with the observations at 420 K representative of stratospheric behavior. At 320 K, the water vapor signal is quite different from that at 420 K, which *Pan et al.* [1997] interpret as related to stratosphere-troposphere exchange.

Figures 5 and 6 show that the air in the altitude range from approximately 330 K to 400 K has ozone concentrations that are characteristic of both the troposphere and the stratosphere in all seasons with the possible exception of autumn. In autumn, profiles have a tropospheric character

to higher altitudes than in other seasons. This is consistent with the LACE observations of long-lived trace gases presented by *Ray et al.* [1998]. During summer, the concentration of ozone in this altitude range is more strongly related to tropopause height than in any other season. At lower altitudes all of the air contains tropospheric values of ozone, and the relationship to tropopause height is unimportant. Similarly, air above 400 K contains stratospheric concentrations of ozone and is not influenced strongly by the height of the tropopause.

The seasonal relationship of the ozone to the tropopause height is, perhaps, surprising. The ozone is more strongly related to undulations in the tropopause height during the summer, when those undulations are smallest. During winter and spring when the synoptic waves are strongest (see Figure 4), the ozone distribution in the high and low tropopause regimes are very similar. This suggests that during winter there is more mixing of air, while during summer transport associated with the raising and lowering of the tropopause with passing synoptic waves is more reversible.

The general circulation paradigm of stratosphere-to-troposphere exchange discussed in *Holton et al.* [1995] usefully describes the mean descent from the stratosphere which supplies the lowermost stratosphere with ozone typical of the stratosphere. However, the transport processes within the lowermost stratosphere are much faster and more complex that those suggested by the mean circulation. Assuming that photochemical production and loss for ozone in the lowermost stratosphere are negligible, this analysis shows that mixing in the lowermost stratosphere occurs in both the latitudinal and vertical planes. If the mixing occurred only in the vertical plane, then the stratospheric ozone profile would appear to be eroded. To the contrary, in winter and spring the ozone in the lowermost stratosphere appears as a bulge of high ozone. This means that ozone values higher than those in the mean vertical profile must be transported in from other latitudes.

Therefore, it is safe to conclude that in the lowermost stratosphere both horizontal and vertical elements of wave transport are important.

This study was originally motivated to help assess the impact of aircraft flying in the lowermost stratosphere on the environment. Earlier work with this model, as well as trajectory studies [*e.g. Schoeberl et al.*, 1998], suggest that aircraft effluent do not reside for long periods of time near the tropopause. Rather, air is transported quickly into the troposphere where many of the aircraft pollutants are then removed. It was noted by *Kawa et al.* [1999] and *Park et al.*, [1999] that compared with two-dimensional models, three-dimensional models showed a weaker correlation of residence time of aircraft pollutants with measures of mean transport processes, such as age of air. This weaker correlation in the three-dimensional model is consistent with the vigorous transport near the tropopause described in this study. This is a process that would not be present in two-dimensional models. Furthermore, it is intuitive that the dynamical undulations that cause the variations studied here could be reversible for ozone transport, but not for aircraft emissions. Since the source of emissions is direct injection into these synoptic features the conservation assumptions of long-lived tracers are not applicable. In is reasonable to conclude from both the observations and three-dimensional model results that two-dimensional models overestimate the lifetime of aircraft effluents in the lowermost stratosphere.

Finally, what does this study tell us about model performance? The model using meteorological information from the assimilation system accurately represents the seasonal cycle of the tropopause and synoptic variability. As time of transport simulation progresses, however, the accumulated errors in the mean transport build up and increasingly degrade the quality of the simulation. The model does show the change in the seasonal cycle that occurs across the altitude range of the lowermost extratropical stratosphere, but does not have as sharp a transition region. The smeared out transition region could be simply related to model resolution, or linked to noise

in the wind fields [*e.g., Gettelman and Sobel,* 1999]. In order to simulate the observed tracer behavior, it is essential that the model accurately represents the tropopause height and the proper relationship between the tropopause and synoptic variability. For the aircraft impact problem, it is important that the altitude of the emissions relative to tropopause be considered when determining the geophysical robustness of assessment calculations.

6. Conclusions

The data presented in this study show that the seasonal behavior of ozone in the lowermost stratosphere is distinctly different from the seasonal behavior in the stratospheric overworld. The sonde data show a marked transition of the seasonal behavior at 400 K, which is about 1.2 km higher than the 380 K surface, the stated upper boundary of the lowermost stratosphere in the *Holton et al.* [1995] review. The HALOE observations are consistent with the sonde observations, though the coarser vertical resolution obscures the sharpness of the transition altitude. The behavior discussed here is similar to the SAGE water vapor and ozone observations presented in *Pan et al.* [1997]. The three-dimensional model, using winds from the GEOS data assimilation system, qualitatively represent the observed behavior, but smoothes the transition between the upper and lower regimes.

These results add another piece of evidence that the atmosphere at and just above the extratropical tropopause is governed by a combination of transport mechanisms. During summer, the rising and falling of the tropopause with passing synoptic waves explains much of the observed variance in the ozone observations. During winter and spring, when the tropopause undulations are stronger, less of the variance is explained by the changes in the tropopause height. We assert, therefore, that there is more effective mixing within the lowermost stratosphere during winter and spring.

This and evidence from other studies, for instance, *Rood et al.* [1997] and *Zahn et al.* [1999], suggest that the extratropical lowermost stratosphere is effectively viewed as a mixed region with the mixing related to tropospheric weather systems. The mixing stirs together air in the lowermost stratosphere that has been supplied by other transport mechanisms such as quasi-isentropic transport from the tropical troposphere as well as descent from above. In addition, as suggested in *Rood et al.* [1997], the storms, themselves, can be effective vehicles of transport. Traveling middle latitude cyclones cause rapid horizontal transport of tropical upper tropospheric air to high latitudes where it then takes on a stratospheric character. Within these traveling cyclones there is also substantial vertical motion from the lower troposphere to the upper troposphere. Since the CO_2 transport results of *Strahan et al.* [1998] show that direct injection across the middle latitude tropopause into the stratosphere does not dominate transport into the lowermost stratosphere, the effect of this vertical transport must be confined very near the tropopause [see also *Hoerling et al.*, 1993; *Grewe and Dameris,* 1996]. However, as the entire region is stirred by the baroclinic waves it all becomes part of a standing mix of air that makes it difficult to determine transport pathways. The transport associated with these baroclinic systems is fully three-dimensional, often having strong diabatic processes which cause transport across isentropic surfaces.

This notion of routine mixing by large-scale dynamical structures is complementary of other recent work, notably *Postel and Hitchman* [1999, see also *Chen,* 1995; *Dunkerton,* 1995]. They point out evidence of large-scale stratosphere-troposphere exchange occurring at summer subtropical latitudes. This exchange is related to Rossby wave mixing, which is ultimately correlated with monsoonal circulations. Further, *Folkins et al.* [1999, amongst others] have identified in the tropics a region, below the tropopause and above 14 km, which contains air with stratospheric ozone, suggesting a mixed region between the troposphere and the stratosphere at

low latitudes. In total, current observations point to a need to reconsider the traditional concepts used to describe the mechanisms of stratosphere-troposphere exchange. Three-dimensional models, such as the one used here, are capable of representing many of the fundamental features of the observations. The increasing demands being made on assessment models motivates us to consider the full three-dimensional and time characteristics of the atmosphere near the tropopause, using fully diabatic models as a tool for organizing and interpreting the complex processes.

Finally, this work was originally motivated by the goal to assess the fate of pollutants from aircraft. It corroborates results of other studies using different techniques [e.g. *Schoeberl et al.*, 1998], which find that mixing processes near the tropopause are significantly faster than in the stratosphere. This helps explain the difference between two- and three-dimensional model assessment studies that were noted in recent reports [e.g. *Kawa et al.*, 1999]. In this case the three-dimensional models, which are reproducing the mean characteristics of the local environment, are probably telling a more geophysically robust story than the highly averaged two-dimensional models, implying that the two-dimensional models overestimate the lifetime of aircraft effluents in the stratosphere.

Acknowledgements

We thank the Goddard Ozone Processing Team for supplying EP-TOMS data. Funding for was research was provided by NASA's Atmospheric Chemistry Modeling and Analysis Program, Atmospheric Effects of Aviation Project, and Earth Observing System Project.

Figure Captions

Figure 1. (a) 1997 time series of Hohenpeissenberg (11 E, 47.8 N) ozonesonde profiles with the seasonal mean removed. Potential temperatures are measured *in situ*. Balloon launch dates are marked with +. (b) Time series of simulated ozone profiles from the chemical transport model (CTM) at (11E, 48 N) with the seasonal mean removed. Dates are that of the balloon launch dates. Potential temperatures are from the GEOS Data Assimilation System. Color scaling is the same for both plots. The lowermost stratosphere is bounded by the 380 K isentrope and the 2 pvu tropopause, both outlined in white.

Figure 2. Probability distribution function (PDF) of modeled ozone at the location of Hohenpeissenberg. The thick line is sampling the model every five days. The cross-hatch is sampling the model every day.

Figure 3. (a) Contour map of Ertel's potential vorticity at 300 hPa on April 4, 1997. Example of low tropopause air (high potential vorticity) is marked by L – high tropopause (low potential vorticity) is marked by H. (b) Same as (a) but for July, 12, 1997. Contour interval is 1 pvu (pvu = 10^{-6} m^2 s^{-1} K kg^{-1}). The 2 pvu contour, which is used to define the tropopause, is in bold. These distributions are characteristic of spring (MAM) and summer (JJA).

Figure 4. (a) Probability distribution function (PDF) of Ertel's potential vorticity at 300 hPa for the 46 N latitude circle for April 4, 1997. (b) Same as (a) but for July 12, 1997.

Figure 5. Ozone PDFs at 350 K for the 42 N to 60 N latitude band taken from the ozonesonde data, the HALOE data, and the model. PDFs are conditional based on the tropopause height at the 300 hPa surface. The high tropopause is the solid line, the low tropopause is dash-dot. Columns from left to right are for winter (DJF), spring (MAM), summer (JJA), and fall (SON). Ozone partial pressure bins are 10 nanobars wide.

Figure 6. Ozonesonde PDFs for summer (JJA) 1991-1996 from the 320 K to the 430 K surface for high tropopause (solid) and low tropopause (dash-dot) conditions. Ozone partial pressure bins are 10 nanobars wide. For display purposes, probabilities greater than 30 % default to 30 %.

Figure 7. Most probable value of ozone on isentropic surfaces as a function of time. Plots are shown for the ozonesondes, HALOE, and the model. Scaling of the z-axis is non-uniform.

Fig. 1a) 1997 Hohenpeissenberg Ozonesondes 47.8N, 11E

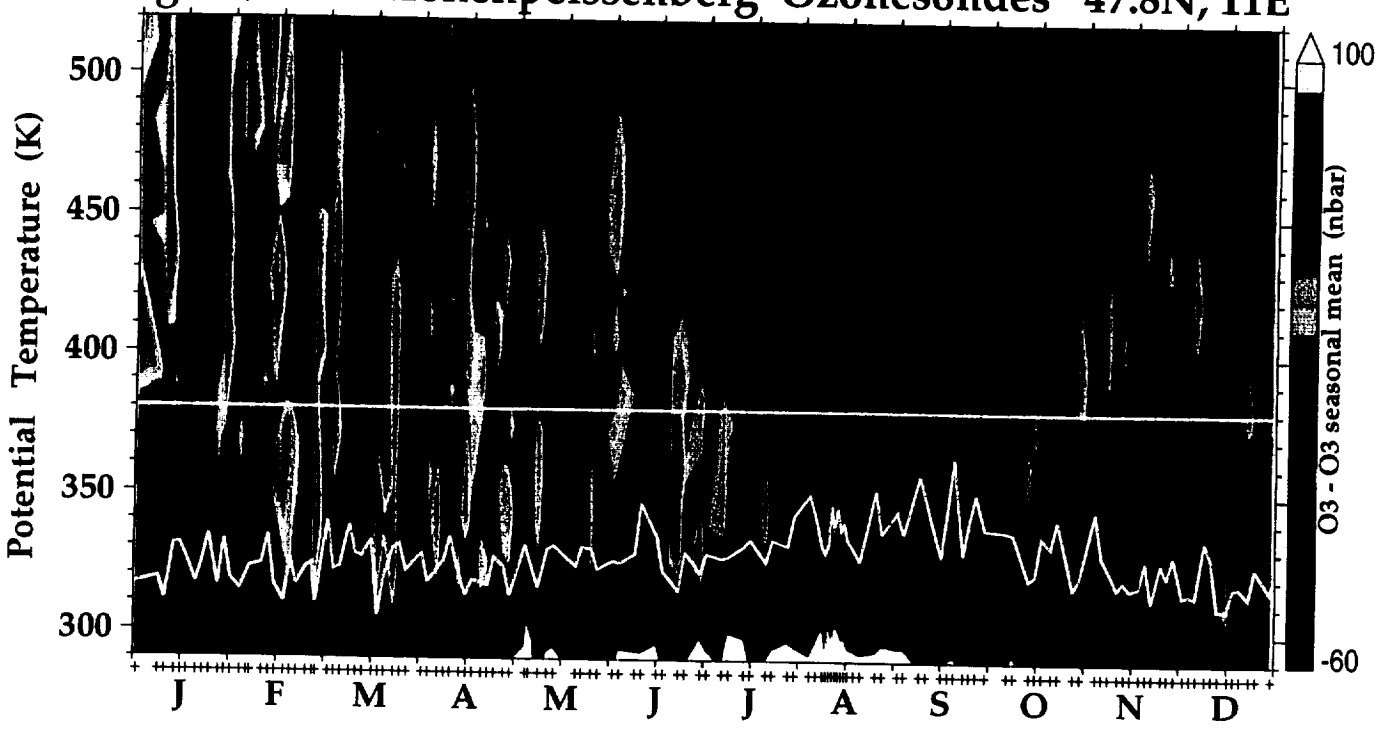

Fig. 1b) 1997 CTM Ozone 48N, 11E

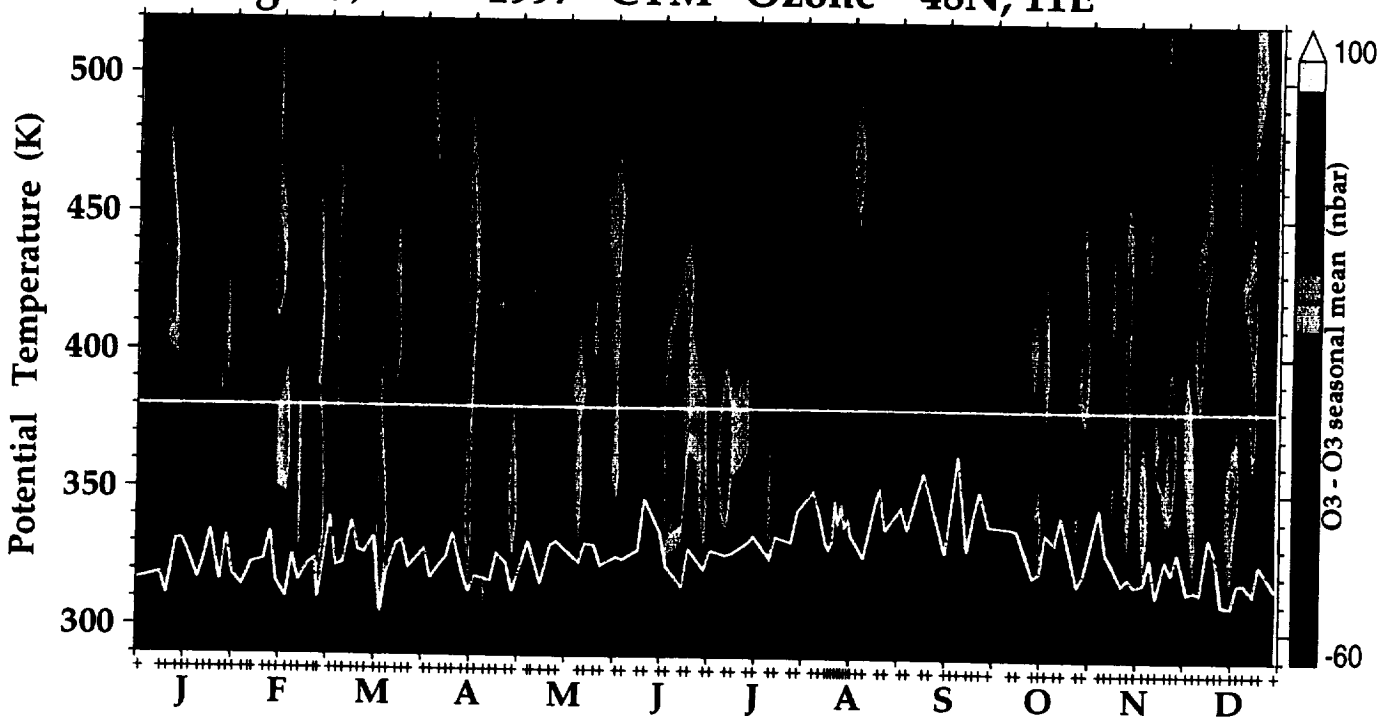

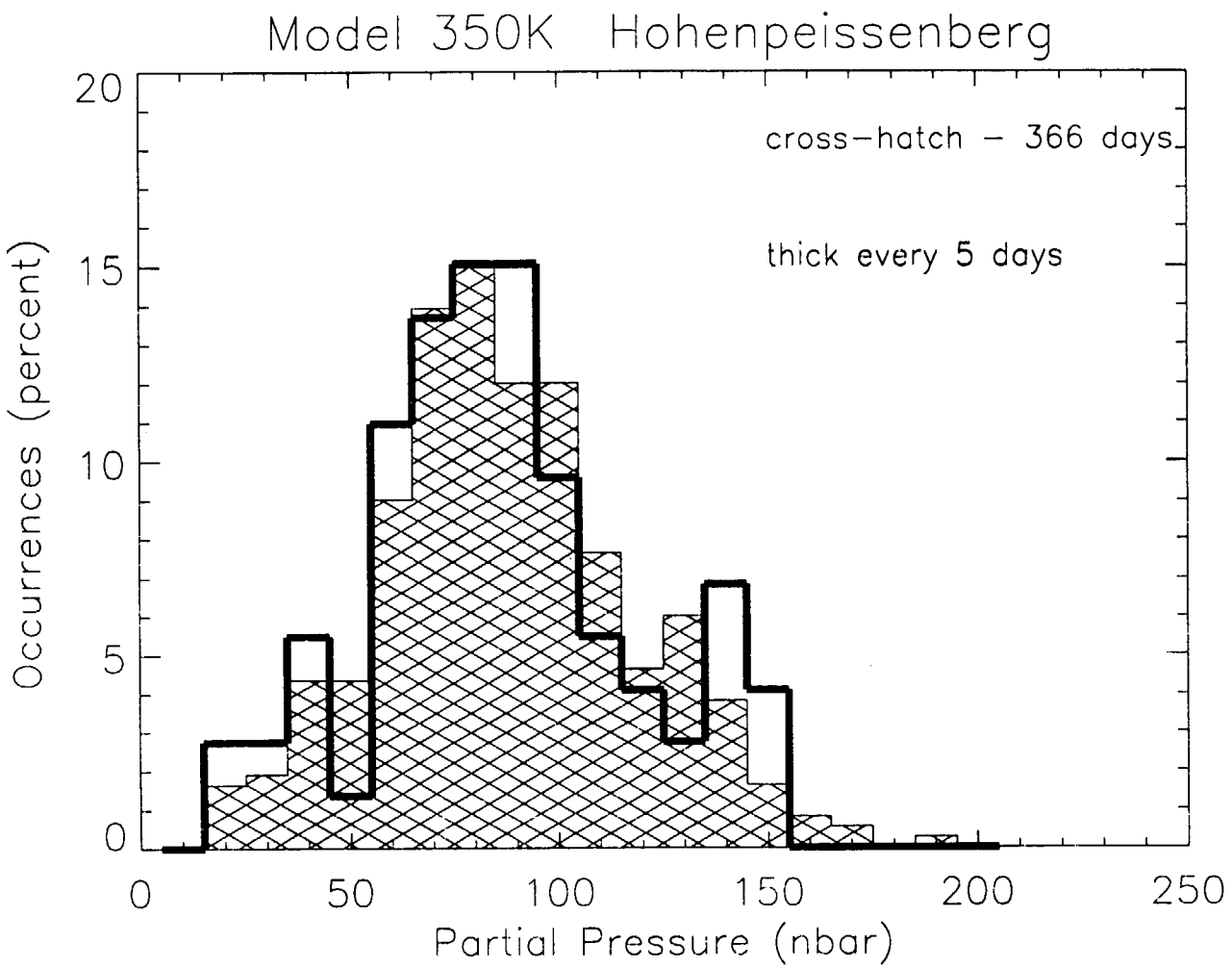
Model 350K Hohenpeissenberg
cross-hatch – 366 days
thick every 5 days
Occurrences (percent)
0
5
10
15
20
0
50
100
150
200
250
Partial Pressure (nbar)

Fig. 3a MAM 970401 GEOS-DAS EPV (pvu) at 300 hPa

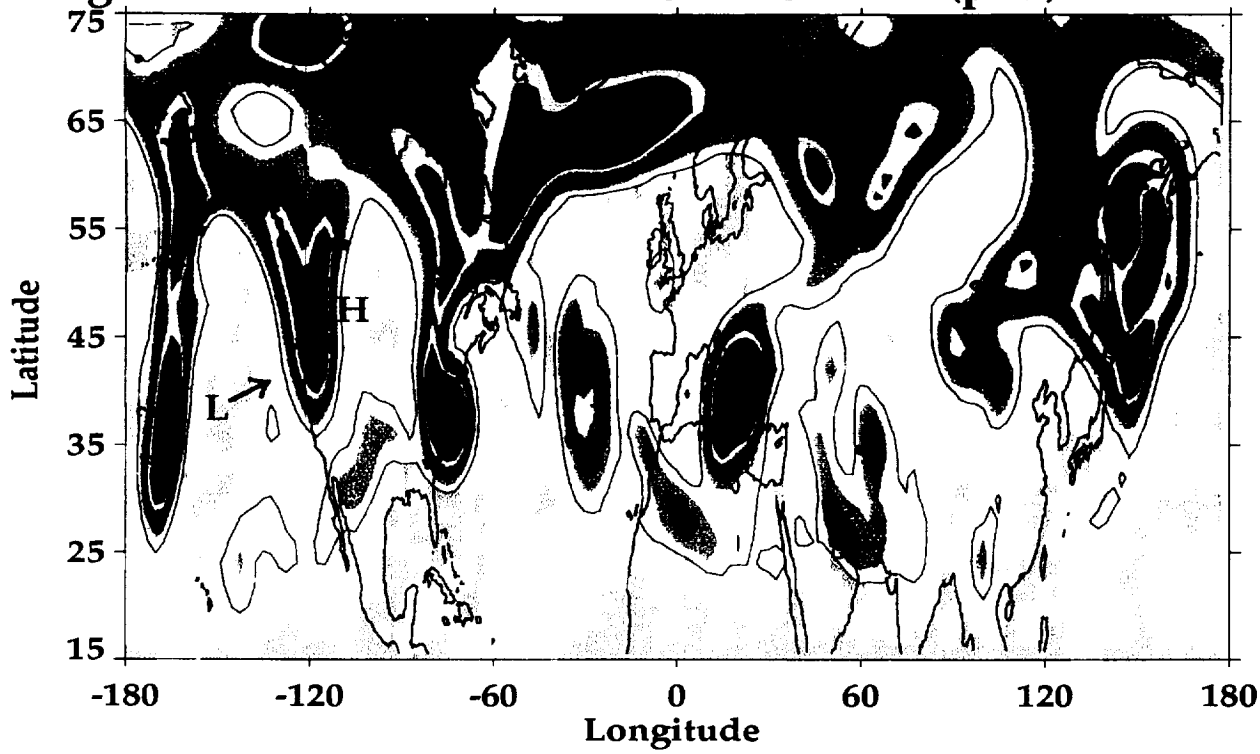

Fig. 3b JJA 970712 GEOS-DAS EPV (pvu) at 300 hPa

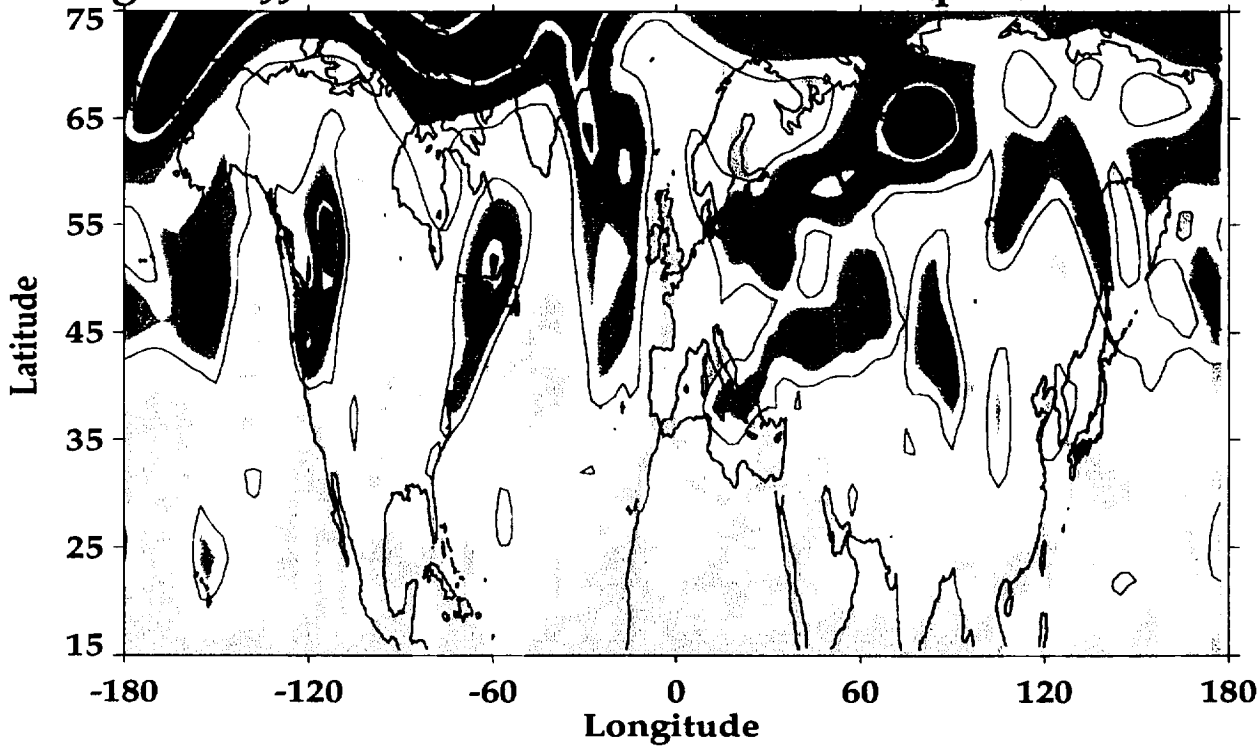

Fig. 4a MAM 970401 EPV PDF at 46N, 300 hPa

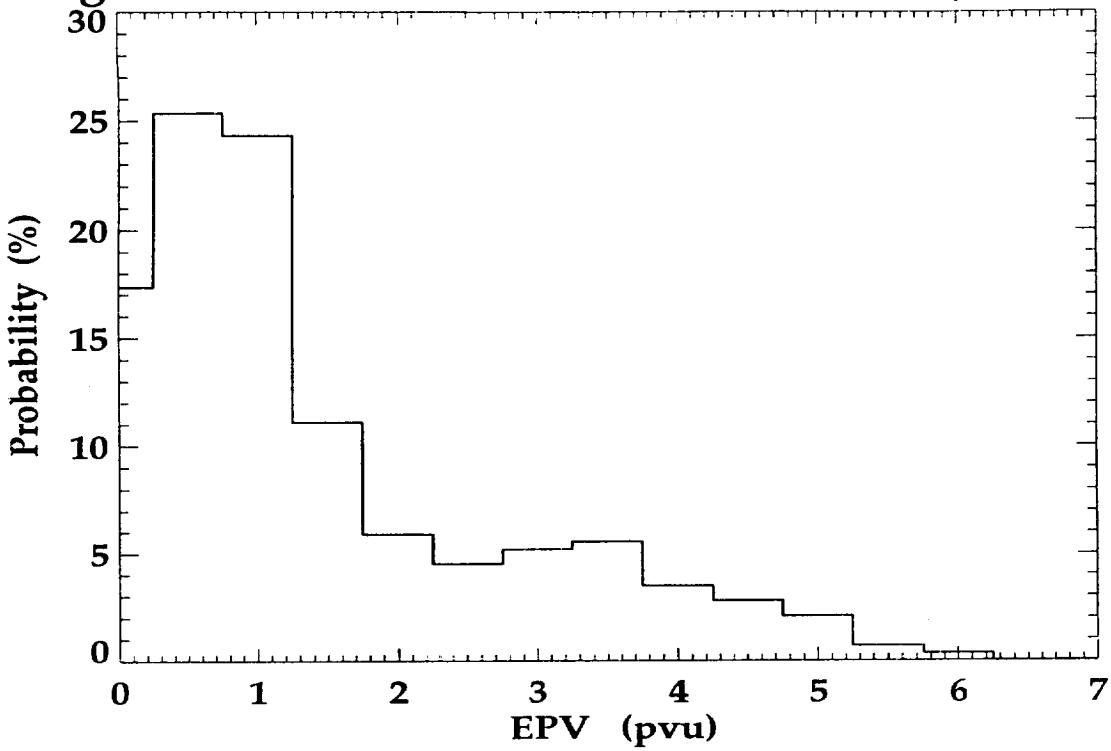

Fig. 4b JJA 970712 EPV PDF at 46N, 300 hPa

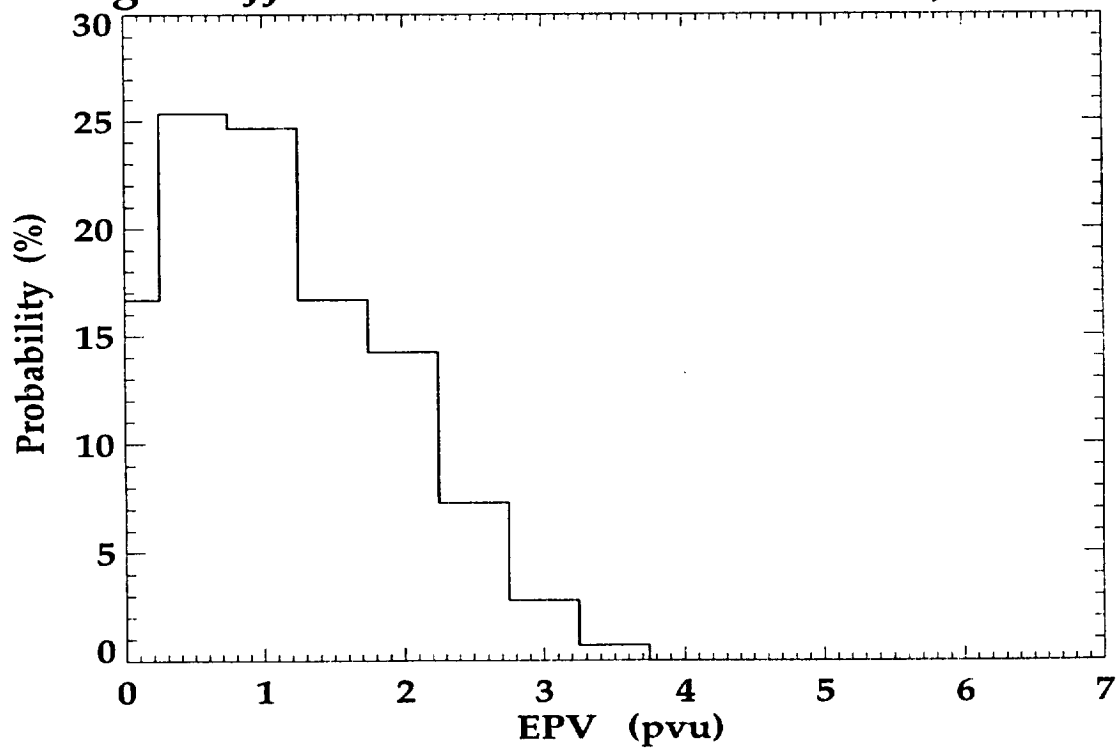

Fig. 5 Seasonal Ozone PDF at 350K 42-60N

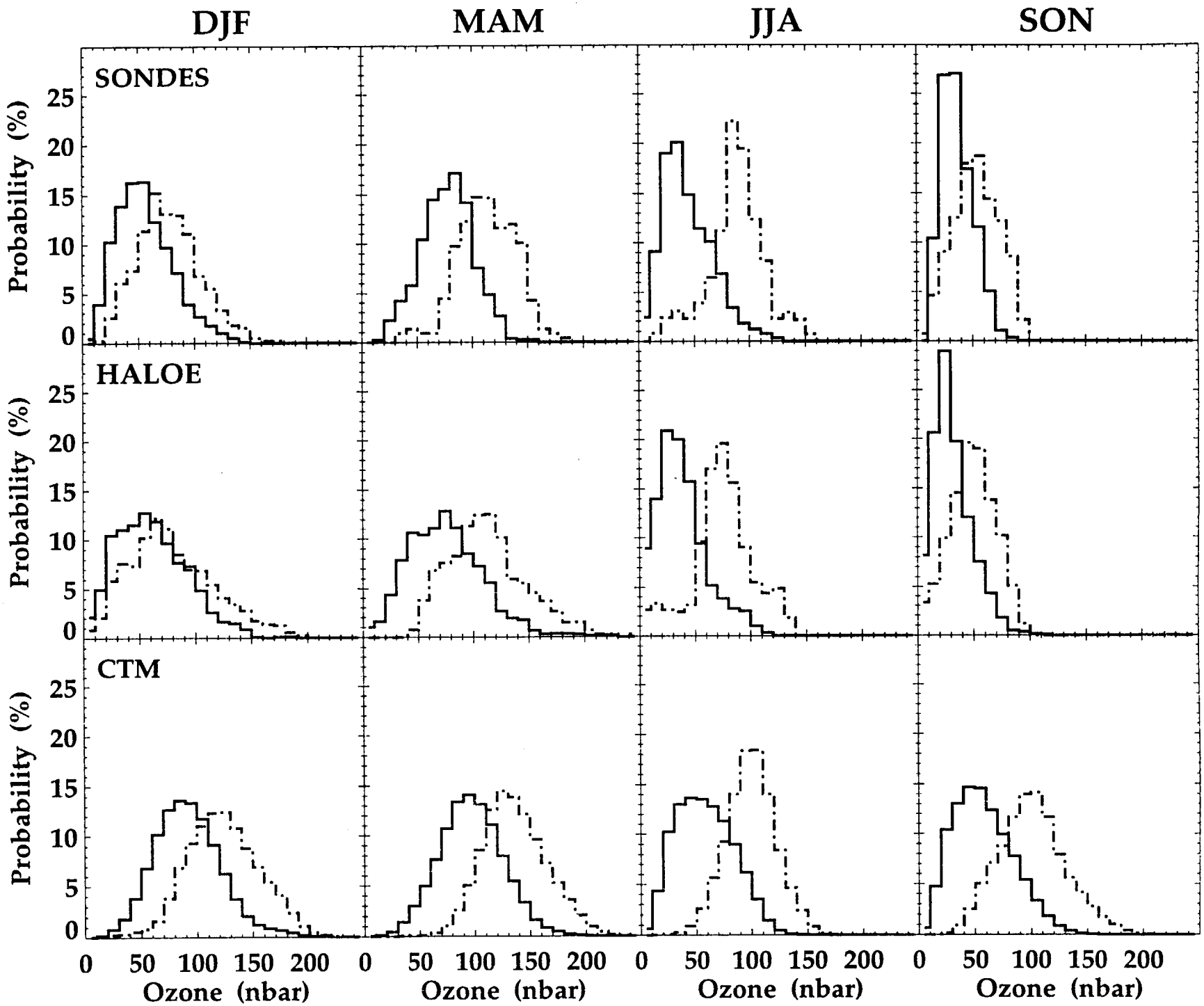

Fig. 6 1991-1996 JJA Ozonesonde PDF 42-60N 320-430K

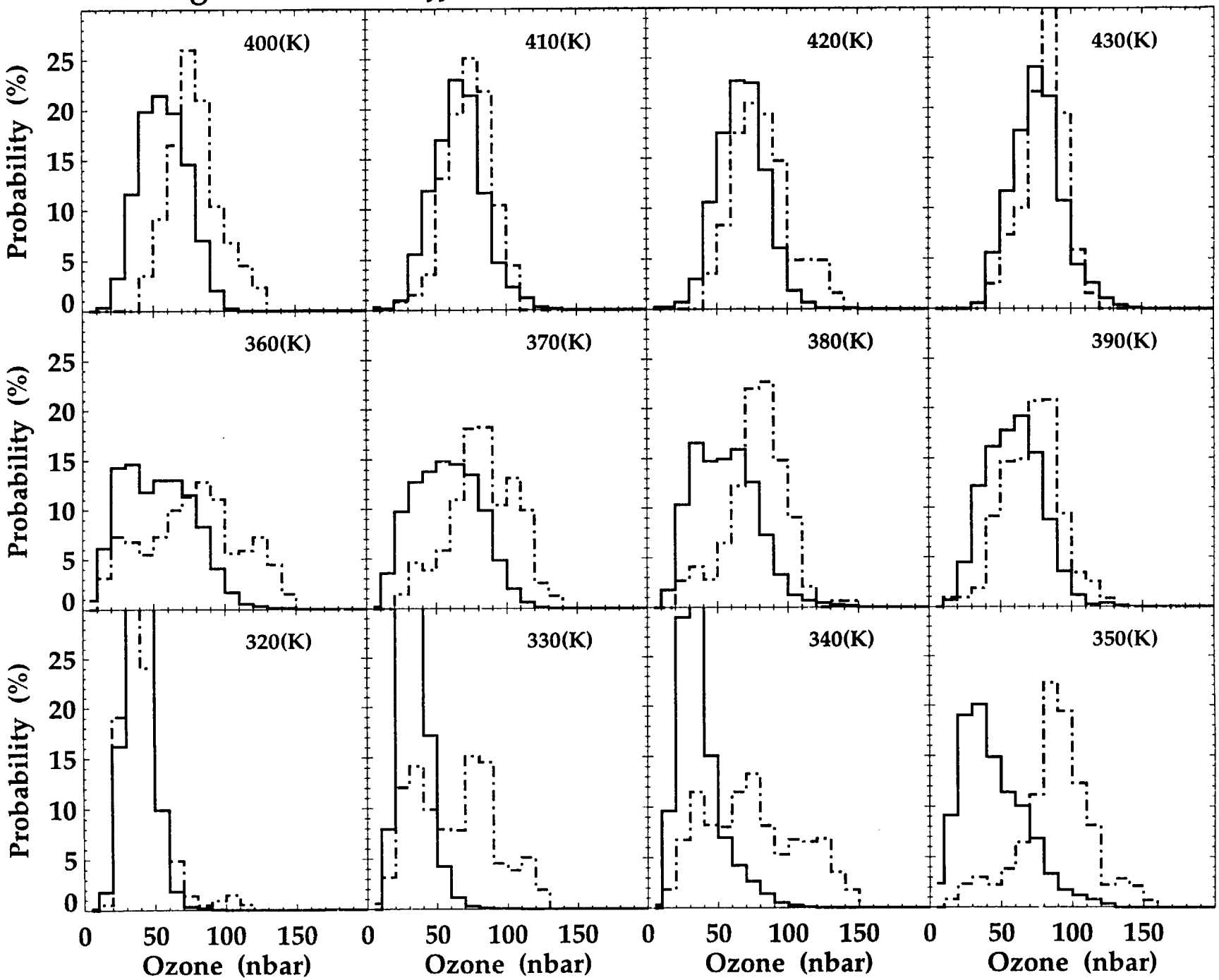

Fig 7a) SONDES Most Probable O3

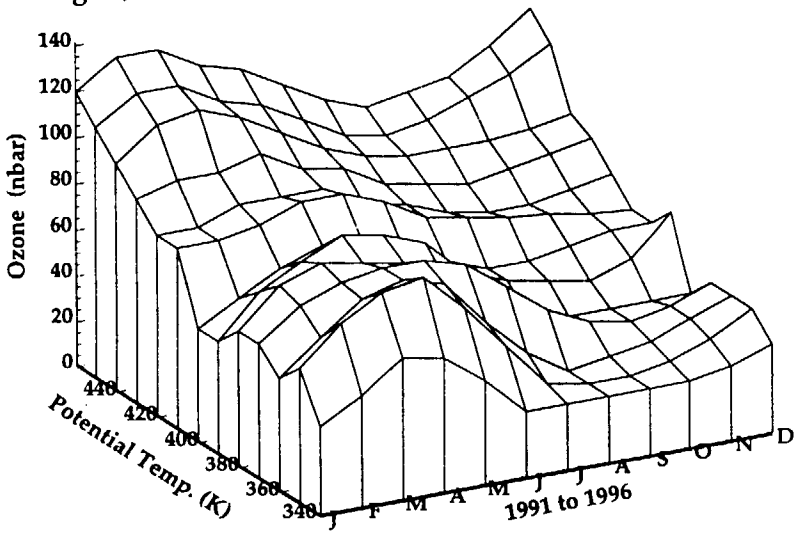

Fig. 7b) HALOE Most Probable O3

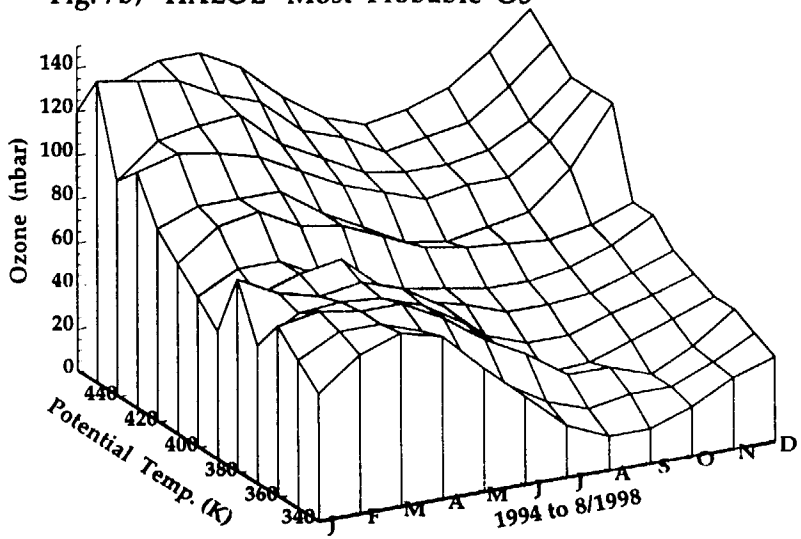

Fig. 7c) CTM Most Probable O3

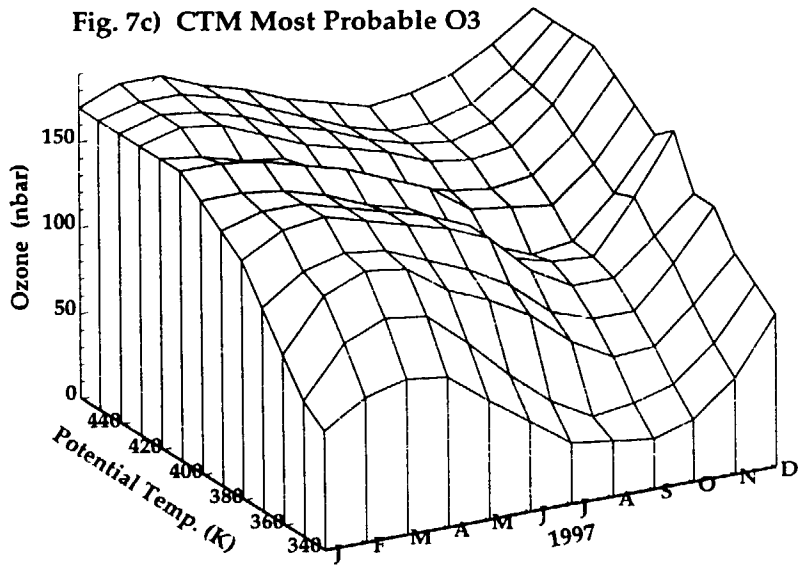

References

Ancellet, G., M. Beekmann, and A. Papayannis, Impact of a cutoff low development on downward transport of ozone in the troposphere, *J. Geophys. Res., 99,* 3451-3468, 1994.

Appenzeller, C., H. C. Davies, and W. A. Norton, Fragmentation of stratospheric intrusions, *J. Geophys. Res., 101,* 1435-1456, 1996a.

Appenzeller, C., J. R. Holton, and K. H. Rosenlof, Seasonal variation of mass transport across the tropopause, *J. Geophys. Res., 101,* 15,071-15,078, 1996b

Bamber, D. J., P. G. W. Healey, B. M. R. Jones, S. A. Penkett, A. F. Tuck, and G. Vaughan, Vertical profiles of tropospheric gases: Chemical consequences of stratospheric intrusions, *Atmos. Environ., 18,* 1759-1766, 1984.

Beekman, M., et al., Regional and global tropopause fold occurrence and related ozone flux across the tropopause, *J. Atm. Chem., 28,* 29-44,1997.

Bethan, S., G. Vaughan, and S. J. Reid, A comparison of ozone and thermal tropopause heights and the impact of tropopause definitions on quantifying the ozone content of the troposphere, *Q. J. R. Meteorol. Soc., 122,* 929-944, 1996.

Bhatt, P. P., E. E. Remsberg, L. L. Gordley, J. M. McInerney, V. G. Brackett, and J. M. Russell III, An evaluation of the quality of Halogen Occultation Experiment ozone profiles in the lower stratosphere, *J. Geophys. Res., 104,* 9261-9275, 1999.

Bruhl, C. et al., Halogen Occultation Experiment ozone channel validation, *J. Geophys. Res., 101,* 10,217-10,240, 1996.

Cerniglia, M. C., R. B. Rood, and A. R. Douglass, Three-dimensional simulation of the influence of a cutoff low on the distribution of northern hemisphere processed air in late January 1992, *J. Geophys. Res., 100,* 16,431-16,443, 1995.

Chen, P., Isentropic cross-tropopause mass exchange in the extratropics, *J. Geophys. Res., 100,* 16,661-16,673, 1995.

Cox, B. D., M. Bithell, and L. J. Gray, A general circulation model study of a tropopause-folding event at middle latitudes, *Q. J. R. Meteorol. Soc., 121,* 883-910, 1995.

Danielsen, E. F., Stratospheric-tropospheric exchange based on radioactivity, ozone and potential vorticity, *J. Atmos. Sci., 25,* 502-518, 1968.

Danielsen, E., R. Bleck, J. Shedlovsky, A. Wartburg, P. Haagenson, and W. Pollock, Observed distribution of radioactivity, ozone, and potential vorticity associated with tropopause folding, *J. Geophys. Res., 75,* 2353-2361, 1970.

Douglass, A. R., C. J. Weaver, R. B. Rood, and L. Coy, A three-dimensional simulation of the ozone annual cycle using winds from a data assimilation system, *J. Geophys. Res., 101,* 1463-1474, 1996.

Douglass, A. R., R. B. Rood, S. R. Kawa and D. J. Allen, A three dimensional simulation of the middle latitude winter ozone in the middle stratosphere, *J. Geophys. Res., 102,* 19,217-19,232, 1997.

Dunkerton, T. J., Evidence of meridional motion in the summer lower stratosphere adjacent to monsoon regions, *J. Geophys. Res., 100,* 16,675-16,688, 1995.

Ebel, A., H. Elbern, J. Hendricks, and R. Meyer, Stratosphere-troposphere exchange and its impact on the structure of the lower stratosphere, *J. Geomag. Geoelectr., 48,* 135-144, 1996.

Folkins, I., M. Loewenstein, J. Podolske, S. J. Oltmans, M. Proffitt, A 14 km mixing barrier in the tropics: Evidence from ozonesondes and aircraft measurements, *J. Geophys. Res.,* to appear, 1999.

Froidevaux, L., et al., Validations of UARS Microwave Limb Sounder ozone measurements, *J. Geophys. Res., 101,* 10,017-10,060, 1996.

Gettelman, A., Lifetimes of aircraft emission in the stratosphere, *Geophys. Res. Lett., 25,* 2129-2132, 1998.

Gettelman, A., and A. H. Sobel, Direct diagnoses of stratosphere–troposphere exchange, *J. Atmos. Sci.,* to appear, 1999.

Grewe, V., and M. Dameris, Calculating the global mass exchange between the stratosphere and troposphere, *Ann. Geophysicae, 14,* 431-442, 1996.

Hall, T. M., D. W. Waugh, K. A. Boering, R. A. Plumb, Evaluation of transport in stratospheric models, *J. Geophys. Res., 104,* 18,815-18,839, 1999.

Hoerling, M. P., T. K. Schaack, and A. J. Lenzen, A global analysis of stratospheric-tropospheric exchange during northern winter, *Mon. Weather Rev., 121,* 162-172, 1993.

Holton, J. R., P. H. Haynes, M. E. McIntyre, A. R. Douglass, R. B. Rood, and L. Pfister, Stratosphere-troposphere exchange, *Rev. Geophys., 33,* 403-439, 1995.

Jackman, C. H., E. L. Fleming, S. Chandra, D. B. Considine, and J. E. Rosenfield, Past, present, and future modeled ozone trends with comparison to observed trends, *J. Geophys. Res., 101,* 28,753-28,767, 1996

Kawa, S. R., et al., *Assessment of the Effects of High-Speed Aircraft in the Stratosphere: 1998,* NASA/TP-1999-20937, 1999.

Kindler, T. P., D. M. Cunnold, F. N. Alyea, W. L. Chameides, G. P. Lou, and K. Schwan, An evaluation using C-14 and N_2O simulations of three-dimensional transport driven by United Kingdom Meteorological Office and Goddard Space Flight Center assimilated winds, *J. Geophys. Res., 103,* 10,827-10,847, 1998

Langford, A. O., C. D. Masters, M. H. Proffitt, E.-Y. Hsie, and A. F. Tuck, Ozone measurements in a tropopause fold associated with a cut-off low system, *Geophys. Res. Lett., 23,* 2501-2504, 1996.

Lamarque, J. F., and P. G. Hess, Cross-tropopause mass exchange and potential vorticity budget in a simulated tropopause folding, *J. Atmos. Sci., 51,* 2246-2269, 1994.

Lin, S. J., and R. B. Rood, Multidimensional flux form semi-Lagrangian transport schemes, *Mon. Weather Rev., 124,* 2046-2070, 1996.

Morgan, M. C., and J. W. Nielsen-Gammon, Using tropopause maps to diagnose weather systems, *Mon. Weather Rev., 126,* 2555-2579, 1998.

Mote, P. W., J. R. Holton, and B. A. Boville, Characteristics of stratosphere-troposphere exchange in a general circulation model, *J. Geophys. Res., 99,* 16815-16829, 1994.

Newman, P. A., and M. R. Schoeberl, A reinterpretation of the data from the NASA stratosphere-troposphere exchange project, *Geophys. Res. Lett., 22,* 2501-2504, 1994.

Pan, L., S. Solomon, W. Randel, J.-F. Lamarque, P. Hess, J. Gille, E.-W. Chiou, and M. P. McCormick, Hemispheric asymmetries and seasonal variations of the lowermost stratospheric water vapor and ozone derived from SAGE II data, *J. Geophys. Res., 102,* 28,177-28,184, 1997.

Park, J. H., M. Ko, C. H. Jackman, and R. A. Plumb, *Models and Measurements II*, 1999

Postel, G. A., and M. H. Hitchman, A climatology of Rossby wave breaking along the subtropical tropopause, *J. Atmos. Sci., 56,* 359-373, 1999.

Price, J. D., *Stratospheric-tropospheric exchange in cut-off-low systems,* Ph. D. thesis, Univ. Coll. of Wales, Aberystwyth, 1990.

Price, J., and G. Vaughan, The potential for stratosphere-troposphere exchange in cut-off-low systems, *Q. J. R. Meteorol. Soc., 119,* 343-365, 1993.

Ray, E.A., F. L. Moore, J. W. Elkins, G. S. Dutton, D. W. Fahey, H. Vomel, S. J. Oltmans, and K. H. Rosenlof, Transport in the northern hemisphere lowermost stratosphere revealed by in situ measurements, *J. Geophys. Res.,* in press, 1999.

Rood, R. B., A. R. Douglass, M. C. Cerniglia, and W. G. Read, Synoptic-scale mass exchange from the troposphere to the stratosphere, *J. Geophys. Res., 102,* 23,467-23,485, 1997.

Russell, J. M. III, L. L. Gordley, J. H. Park, S. R. Drayson, W. D. Hesketh, R. J. Cicerone, A. F. Tuck, J. E. Frederick, J. E. Harries, and P. J. Crutzen, The Halogen Occultation Experiment, *J. Geophys. Res., 98,* 10,777-10,798, 1993

Schoeberl, M. R., C. H. Jackman, and J. E. Rosenfield, A Lagrangian estimate of aircraft effluent lifetime, *J. Geophys. Res., 103,* 1998.

Schubert, S. D., R. B. Rood, and J. Pfaendtner, An assimilated dataset for earth science applications, *Bull. Am. Meteorol. Soc., 74,* 2331-2342, 1993.

Shapiro, M. A., Turbulent mixing within tropopause folds as a mechanism for the exchange of chemical constituents between the stratosphere and the troposphere, *J. Atmos. Sci., 37,* 994-1004, 1980.

Sparling, L. C., Statistical perspectives on stratospheric transport, *J. Geophys. Res.,* submitted, 1999.

Strahan, S. E., A. R. Douglass, J. E. Nielsen, K. A. Boering, The CO2 seasonal cycle as a tracers of transport, *J. Geophys. Res., 103,* 13,729-13,741, 1998.

Van Haver, P., D. De Muer, M. Beekmann, and C. Mancier, Climatology of tropopause folds at midlatitudes, Geophys. Res. Lett., 23, 1033-1036, 1996.

Vaughan, G., and J. D. Price, Ozone transport into the troposphere in a cut-off low event, *Ozone in the Atmosphere,* R. D. Bojkov and P. Fabian [eds.], pp.415-418, A. Deepak, Hampton, Va., 1989.

Waugh, D. W., Seasonal variation of isentropic transport out of the tropical stratosphere, *J. Geophys. Res., 101,* 4007-4023, 1996.

Weaver, C. J., A. R. Douglass, and R. B. Rood, Lamination frequencies as a diagnostic for horizontal mixing in a 3D transport model, *J. Atmos. Sci.,* to appear, 1999.

Zahn, A., R. Neubert, M. Maiss, and U. Platt, Fate of long-lived trace species near the Northern Hemispheric tropopause: Carbon dioxide, methane, ozone, and sulfur hexafluoride, *J. Geophys. Res., 104,* 13,923-13,942, 1999.